

## Supplementary Information

### Opto-Thermophoretic Manipulation of Colloidal Particles in Non-Ionic Liquids

Xiaolei Peng<sup>1#</sup>, Linhan Lin<sup>1,2#</sup>, Eric H. Hill<sup>1,2</sup>, Pranaw Kunal<sup>3</sup>, Simon M. Humphrey<sup>3</sup>, and

Yuebing Zheng<sup>1,2,\*</sup>

<sup>1</sup>Materials Science & Engineering Program and Texas Materials Institute, The University of Texas at Austin, Austin, TX 78712, USA.

<sup>2</sup>Department of Mechanical Engineering, The University of Texas at Austin, Austin, TX 78712, USA.

<sup>3</sup>Department of Chemistry, The University of Texas at Austin, Austin, TX 78712, USA.

\*E-mail: [zheng@austin.utexas.edu](mailto:zheng@austin.utexas.edu)

# These authors contributed equally to this work.

## Supplementary Videos

**Video S1:** Trapping and anti-trapping of a 1  $\mu\text{m}$  polystyrene (PS) sphere in water and methanol, respectively. The “+” indicates the laser beam spot.

**Video S2:** Trapping and anti-trapping of a 2  $\mu\text{m}$  PS sphere in water and methanol, respectively. The “+” indicates the laser beam spot.

**Video S3:** Release of a 1  $\mu\text{m}$  hydrophilic silica sphere in water when translating it from an optothermal substrate to a glass substrate. The “+” indicates the laser beam spot.

**Video S4:** Transport and rotation of Ag nanowires (AgNWs) in IPA. The frame rate is 3 times of the original one.

## Supplementary Figures

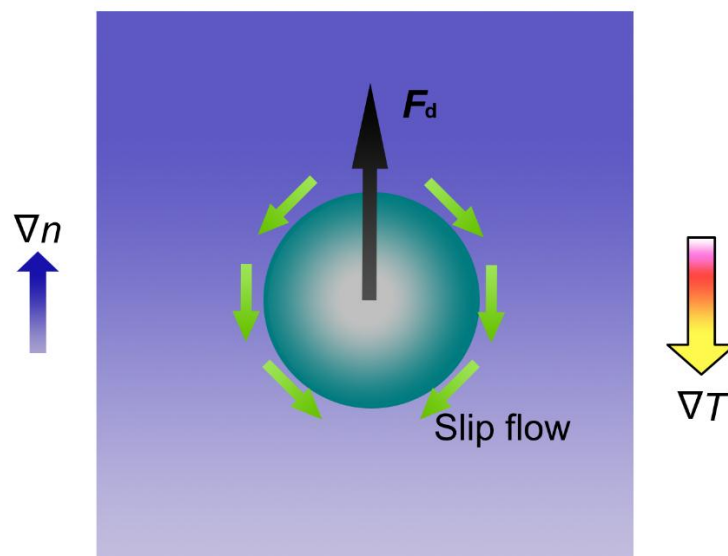


**Figure S1:** The dispersion force  $F_d$  originates from a density gradient of the solvent  $\nabla n$  induced by the temperature gradient field  $\nabla T$ . In the particle frame of reference, a slip flow from the cold to hot region occurs at the particle surface. In the laboratory frame of reference, the particle migrates from the hot to the cold region.

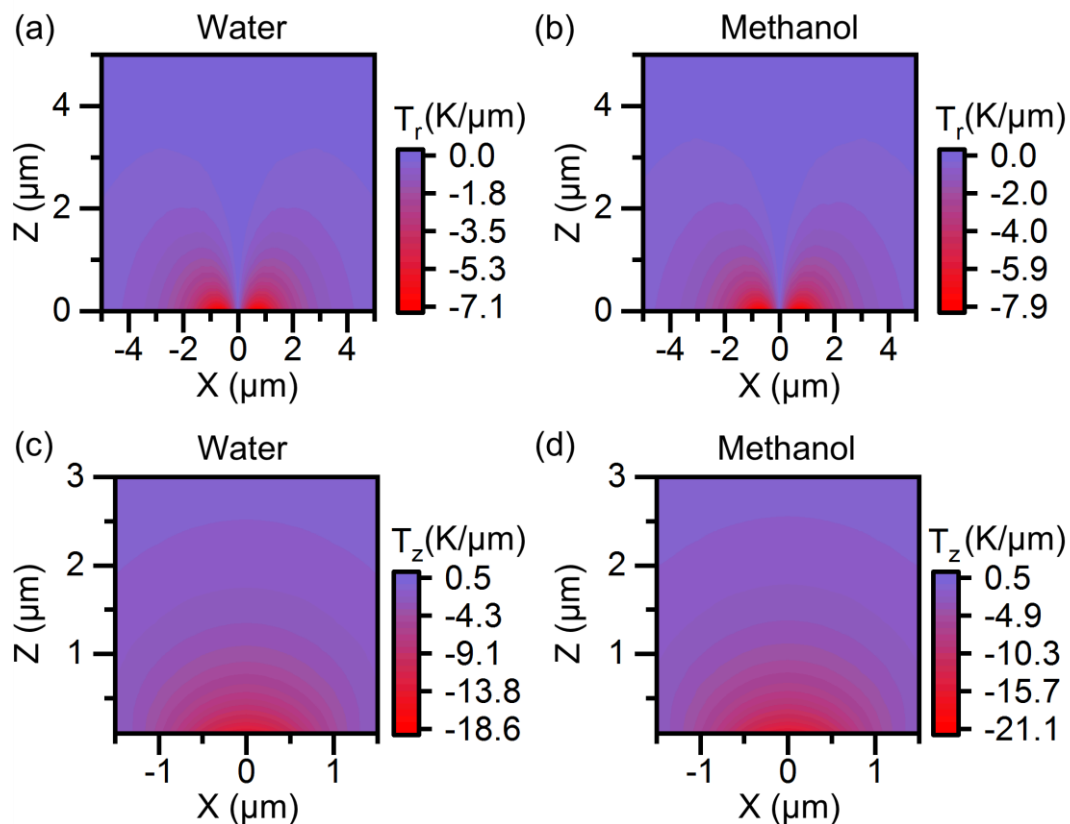


**Figure S2:** Cross-sectional maps of the temperature gradient field  $T_r$  (x-y plane or in-plane) and  $T_z$  (z direction) at the substrate-solvent interface where a laser beam with a diameter of  $2\ \mu\text{m}$  and a power intensity of  $0.16\ \text{mW}/\mu\text{m}^2$  is illuminated onto the substrate beneath a  $20\ \mu\text{m}$  thick chamber that contains (a, c) water and (b, d) methanol.

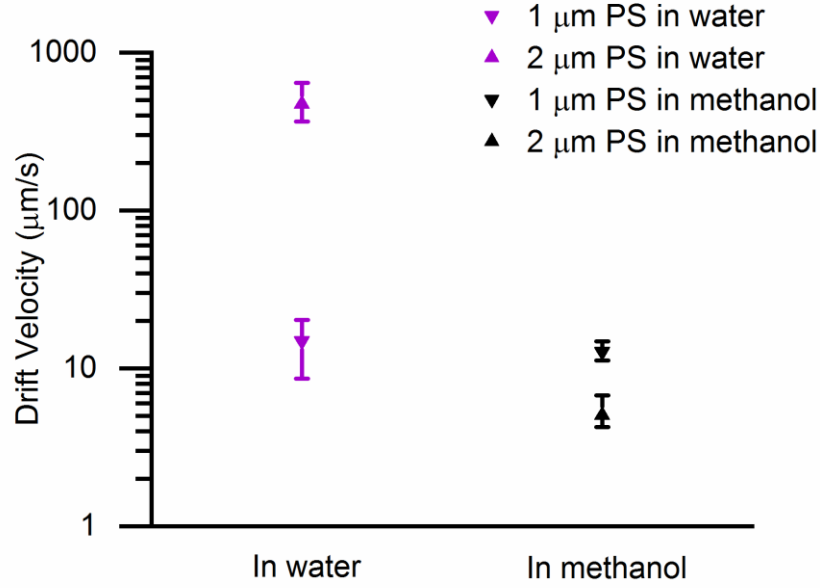


**Figure S3:** Drift velocities of 1  $\mu\text{m}$  and 2  $\mu\text{m}$  PS particles under a light-generated temperature gradient field in water and methanol. Particles in water drift from the cold to the hot region (*i.e.*, trapping) while particles in methanol drift from the hot to the cold region (*i.e.*, anti-trapping). A laser beam with a diameter of 2  $\mu\text{m}$  and a power intensity of 0.16  $\text{mW}/\mu\text{m}^2$  was focused onto the optothermal substrate to create the localized temperature gradient field.

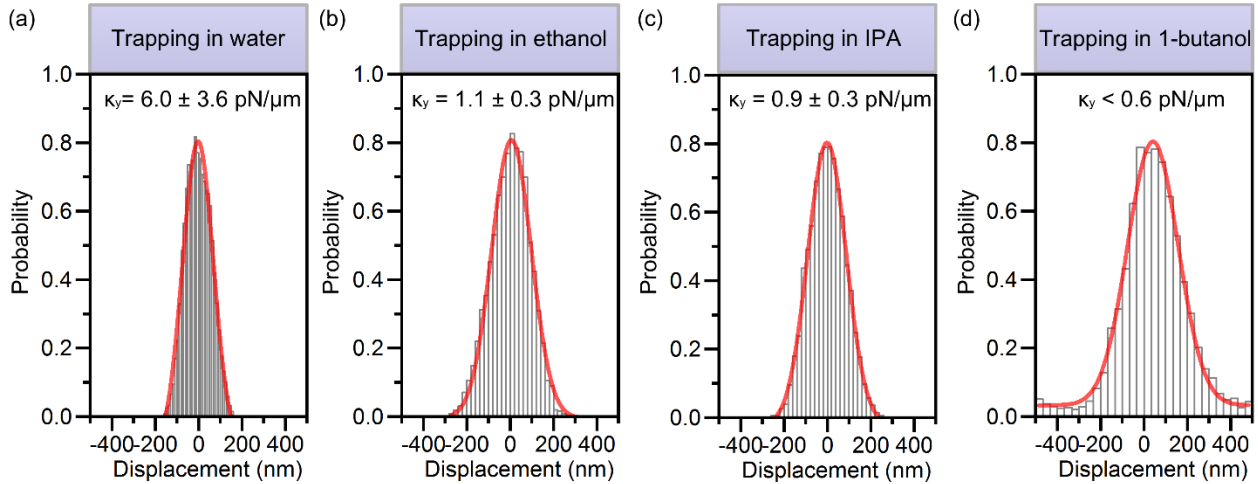


**Figure S4:** Measured histograms of particle displacement and the corresponding trapping stiffness ( $y$  direction) for 500 nm PS spheres under the temperature gradient field in (a) water, (b) ethanol, (c) IPA and (d) 1-butanol.

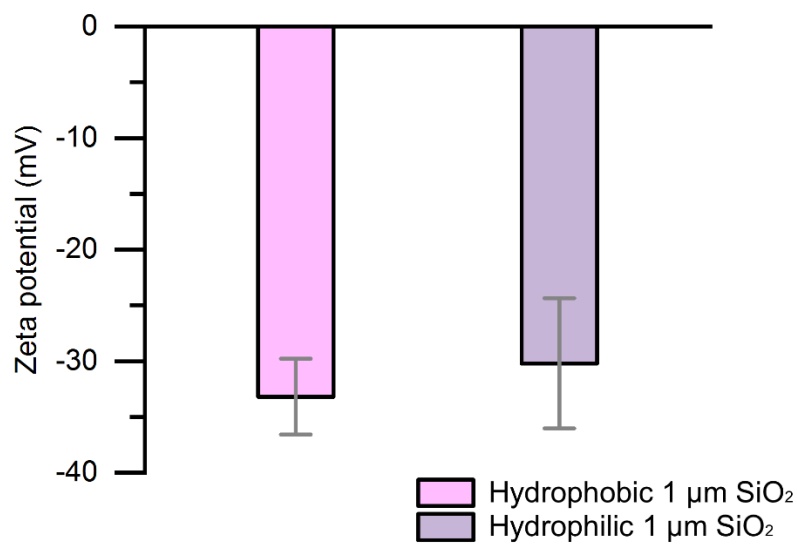


**Figure S5:** Zeta potentials of 1 μm hydrophobic and hydrophilic silica (SiO<sub>2</sub>) particles in water.

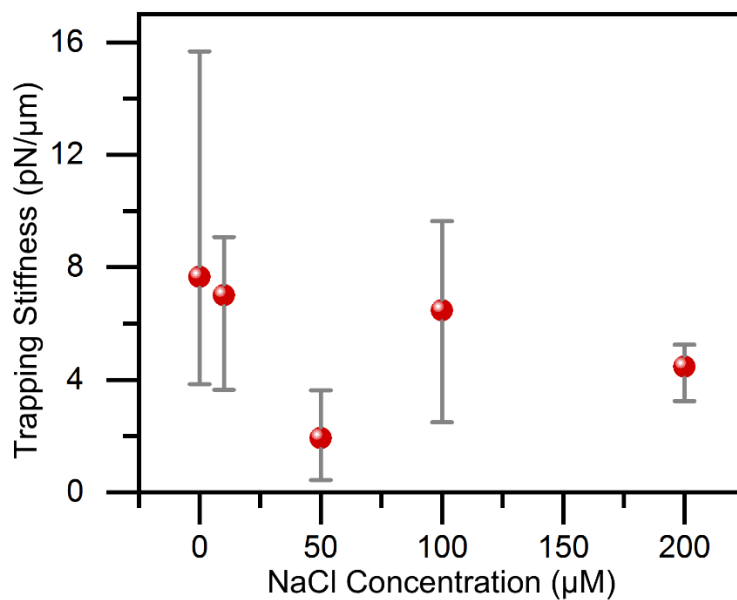


**Figure S6:** Measured trapping stiffness for 500 nm PS spheres in water as a function of NaCl concentration.

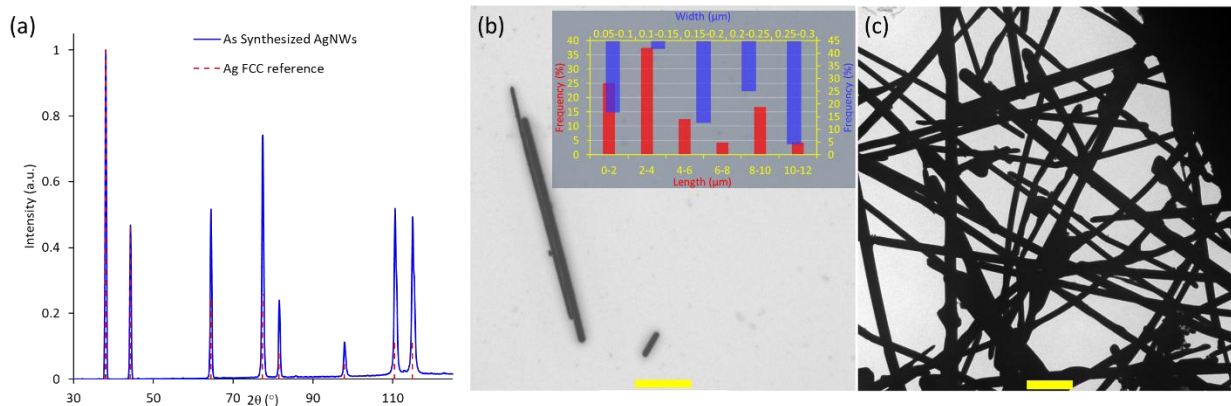


**Figure S7:** (a) Powder X-ray diffraction spectrum of as-synthesized AgNWs, showing face-centered cubic (FCC) structure. (b-c) Transmission electron micrographs of AgNWs. Inset in (b) shows length (bottom-left axis) and width (top-right axis) distributions of the AgNWs. Scale bars in (b) and (c) are 2  $\mu\text{m}$  and 1  $\mu\text{m}$ , respectively.

## Supplementary Table

**Table S1.** Parameters for calculation of  $D_T$  in different solvents at 25  $^{\circ}\text{C}$  ( $\kappa_p$  is 0.03  $\text{W m}^{-1} \text{K}^{-1}$ ).

Solvents	$\epsilon_b$	$\eta$ (cP)	$\kappa$ ( $\text{W m}^{-1} \text{K}^{-1}$ )	$\frac{\epsilon_b}{\eta T} \frac{2\kappa}{2\kappa + \kappa_p}$ ( $\text{cP}^{-1} \cdot \text{K}^{-1}$ )
Water	78.5	1.082	0.606	0.118
Methanol	31.5	0.545	0.198	0.090
Ethanol	24.3	0.890	0.159	0.042
IPA	18.0	1.960	0.136	0.014
1-butanol	17.3	2.544	0.155	0.011